

JGR Biogeosciences

RESEARCH ARTICLE

10.1029/2023JG007812

Key Points:

- Riverine organic carbon is compositionally distinct in source and signature during the freshet compared to other stages of the hydrograph
- During the freshet, there is preferential loss of lignin compared to bulk dissolved organic carbon across a landto-ocean salinity gradient
- Lignin-chromophoric dissolved organic matter relationships vary across Yukon interfaces (river to delta, plume water to high salinity)

Supporting Information:

Supporting Information may be found in the online version of this article.

Correspondence to:

A. J. Burns, ajburns@ucdavis.edu

Citation:

Burns, A. J., Spencer, R. G. M., Kellerman, A. M., Yan, G., Leonard, L., Kaiser, K., et al. (2024). The distinct composition and transformation of terrestrial organic carbon in the Yukon River delta and plume during the mighty spring freshet. *Journal of Geophysical Research: Biogeosciences*, 129, e2023JG007812. https://doi.org/10.1029/2023JG007812

Received 20 SEP 2023 Accepted 2 JUN 2024

© 2024. The Author(s). This is an open access article under the terms of the Creative Commons Attribution-NonCommercial-NoDerivs License, which permits use and distribution in any medium, provided the original work is properly cited, the use is non-commercial and no modifications or adaptations are made.

The Distinct Composition and Transformation of Terrestrial Organic Carbon in the Yukon River Delta and Plume During the Mighty Spring Freshet

A. J. Burns¹, R. G. M. Spencer², A. M. Kellerman², G. Yan³, L. Leonard³, K. Kaiser³, A. Mannino⁴, M. Tzortziou⁵, and P. J. Hernes¹

¹Department of Land, Air and Water Resources, University of California, Davis, Davis, CA, USA, ²National High Magnetic Field Laboratory Geochemistry Group, Department of Earth, Ocean, and Atmospheric Science, Florida State University, Tallahassee, FL, USA, ³Department of Marine and Coastal Environmental Science, Texas A&M University, Galveston, TX, USA, ⁴Ocean Ecology Laboratory (Code 616), NASA Goddard Space Flight Center, Greenbelt, MD, USA, ⁵Earth and Atmospheric Sciences Department, The City College of New York, New York, NY, USA

Abstract Arctic amplification is leading to increased terrestrial organic carbon (terrOC) mobilization with downstream impacts on riverine and marine biogeochemistry. To improve quantification and characterization of terrOC discharged to the Arctic Ocean, Yukon River delta samples were collected during three stages of the annual hydrograph (ascending limb/peak freshet, descending limb, late summer) and across a land-to-ocean salinity gradient (0.08–29.06 ppt). All samples were analyzed for dissolved organic carbon (DOC) concentration and lignin phenols to determine seasonal variability in riverine terrOC and salinity-induced transformation of highly aromatic terrestrial compounds. Additionally, the relationship between lignin and absorbance at 350 and 412 nm was assessed to determine the feasibility of using optical proxies for accurate quantification, both seasonally and across expansive salinity gradients. Lignin phenols were highest during the ascending limb/peak freshet (0.58-0.97 mg/100 mg OC) when riverine DOC was dominated by young vascular plant sources, whereas lignin phenols were lower (0.15-0.89 mg/100 mg OC) and riverine DOC more variable in terrestrial source and diagenetic state during the descending limb and late summer. Across the sampled salinity gradient, there was disproportionate depletion of lignin (up to 73%) compared to DOC (up to 22%). Finally, while optical proxies can be used to quantify lignin within seasonal or spatial contexts, increased uncertainty is likely when expanding linear correlations across Arctic land-ocean continuums. Overall, results indicate seasonal, spatial, interannual, and climatic controls that are amplified during high-flow conditions and important to constrain when investigating Arctic terrOC cycling and land-ocean DOC flux.

Plain Language Summary The Arctic is experiencing an amplified warming phenomenon that is driving a variety of landscape changes. Through these landscape transformations, large amounts of organic carbon can be transported to nearby rivers. However, the fate and transport of organic carbon along Arctic land-ocean continuums is largely unknown, primarily due to simultaneous complex processes that occur in deltas and coastal zones. To improve the quantification of landscape-derived dissolved organic carbon (DOC) transported from the land to the Arctic Ocean, surface water samples were collected throughout the Yukon River delta (Alaska, USA) during three distinct seasons and across a land-ocean salinity gradient extending from freshwater to high-salinity water. To measure riverine organic carbon coming from the landscape, we analyzed all samples for DOC and an environmental biomarker that is specific to terrestrial sources (lignin phenols). Lignin concentrations and compositions were used to determine seasonal differences in the magnitude and type of terrestrial inputs, as well as coastal processing of organic carbon. Results show spatial and seasonal differences in DOC concentration and composition within the Yukon River delta and coastal zone that highlight the complexity of carbon cycling in Arctic regions.

1. Introduction

The Arctic is warming two to four times faster than the rest of the globe, leading to pronounced landscape changes and the potential for widespread effects on local riverine and marine biogeochemistry (e.g., Meredith et al., 2019; Rantanen et al., 2022; Schuur et al., 2015). This amplified climate warming phenomenon is driving a variety of Arctic processes (Box et al., 2019) including permafrost thaw, coastal erosion, shifting hydrologic flows, increased precipitation (Rapaic et al., 2015; Rawlins et al., 2010), intensifying riverine discharge (e.g., Haine

BURNS ET AL. 1 of 17

et al., 2015; Holmes et al., 2015; Rawlins et al., 2010) and changes to land cover (Bhatt et al., 2017)—all of which are expected to influence the concentration and composition of terrestrial organic carbon (terrOC) transported along Arctic land-ocean continuums. The majority of terrOC is exported from Arctic watersheds as dissolved organic carbon (DOC) (e.g., Holmes et al., 2012; McClelland et al., 2016; Spencer et al., 2015), which, depending on the composition and associated reactivity, influences microbial networks and light-absorbing properties. Biolabile forms of DOC (e.g., aliphatics, carbohydrates) are microbially respired and can be released as CO₂ (Polimene et al., 2022; Spencer et al., 2015; Vonk et al., 2013), whereas chromophoric DOC (e.g., aromatics) absorbs solar radiation (Chang & Dickey, 2004; Pegau, 2002) and attenuates sunlight needed for photodegradation of stable DOC (Grunert et al., 2021; Ward et al., 2017) and phytoplankton primary production (Clark et al., 2022). While previous studies have estimated Arctic land-ocean DOC flux based on riverine measurements taken above the heads of tides (e.g., Holmes et al., 2012; Raymond et al., 2007; Spencer et al., 2009), there are still several uncharacterized regions that can significantly impact biogeochemical inputs and cycling at the land-ocean interface such as large river deltas and river plumes. Thus, there is a dearth of knowledge surrounding the deltaic and coastal transformation of terrOC that ultimately limits accurate quantification of terrOC that enters the Arctic Ocean under current and future warming scenarios.

The Yukon River hosts one of the largest deltas in the world and is capable of transforming terrOC across this vast land-ocean continuum through chemical overprinting (Eckard et al., 2007, 2020), photodegradation (Grunert et al., 2021), microbial processing (Clark & Mannino, 2021), and salinity-induced flocculation (Asmala et al., 2014; Sholkovitz, 1976). Based on these simultaneous and distinct transformation processes, there is expected spatial heterogeneity in the composition of terrOC measured across the Yukon River delta and plume compared to upstream riverine samples. Previous studies have focused on characterizing sites at, or upstream of, the USGS gaging site at Pilot Station (located ~200 km from the Yukon River mouth), investigating seasonal and spatial variability in upstream riverine composition (Aiken et al., 2014; Spencer et al., 2008, 2009) compared to other major Arctic rivers (Amon et al., 2012; Mann et al., 2016). While this data and historical information is beneficial in informing our understanding of upstream processes and biogeochemical seasonality of the Yukon River, it is clear that there needs to be further characterization of terrOC downstream and into the coastal zone if we are to understand Arctic terrOC cycling and land-ocean DOC flux.

Variability in terrOC composition can be elucidated through the quantification of lignin phenols, a biogeochemical tracer and environmental biomarker. In terrestrial-dominant systems like the Yukon (Raymond et al., 2007; Striegl et al., 2005), DOC and chromophoric dissolved organic matter (CDOM) can be used to investigate terrOC cycling within the river system, but there are limitations when extending measurements into coastal zones. In these relatively uncharacterized regions, particularly in the Arctic, there may be in situ production of optically-active marine carbon that is indistinguishable from terrestrial sources when using bulk organic carbon measurements (Chen et al., 2002, 2004)—necessitating the use of terrestrial-specific biomarkers to understand terrOC transport and transformation across Arctic land-ocean continuums. Dissolved lignin phenols are optically active compounds that originate from vascular plants but are prominent in environmental systems due to their stability over shorter environmentally-relevant timescales (Opsahl & Benner, 1997), allowing them to be unambiguous indicators of terrestrial influence (Hedges & Mann, 1979). Compared to other terrestrial tracers, such as cutin or use of stable isotopes, lignin offers greater analytical utility due to lower rates of reactivity and species-specific composition in all vascular plant types (Cloern et al., 2002; Opsahl & Benner, 1995). Given that ubiquity, and molecular-level source variability, separating lignin into distinct chemical groups (p-hydroxy, cinnamyl, syringyl, and vanillyl phenols; and acid, aldehyde, and ketone compounds) can indicate terrOC sources and diagenetic state, which further informs our understanding of riverine composition and its control on fate and transport processes.

In this study, we characterized dissolved lignin phenols throughout the Yukon River delta during three stages of the annual hydrograph to determine seasonal variability in terrOC composition. Additionally, we quantified dissolved lignin phenols across an expansive salinity gradient (n=17) extending from freshwater (0.08 ppt) to high salinity marine (29.06 ppt) waters to evaluate terrOC transformation within the Yukon River plume during the ascending limb/peak freshet. Lignin and DOC concentrations were compared to conservative mixing to investigate whether the aromatic nature of dissolved lignin resulted in mixing behavior that deviated from the DOC pool. Finally, we compared lignin concentration to absorbance at 350 nm (a_{350}) and 412 nm (a_{412}) to evaluate whether established linear relationships permit the use of optical proxies for quantification of complex chemical compounds along Arctic land-ocean continuums. We hypothesize that rapid water transport during the

BURNS ET AL. 2 of 17

21698961, 2024, 6, Downloaded from https://agupubs.onlinelibrary.wiley.com/doi/10.1029/2023JG007812, Wiley Online Library on [24/08/2024]. See the Terms and Conditions (https://onlinelibrary.wiley.com/doi/10.1029/2023JG007812, Wiley Online Library on [24/08/2024]. See the Terms and Conditions (https://onlinelibrary.wiley.com/doi/10.1029/2023JG007812, Wiley Online Library on [24/08/2024]. See the Terms and Conditions (https://onlinelibrary.wiley.com/doi/10.1029/2023JG007812, Wiley Online Library on [24/08/2024]. See the Terms and Conditions (https://onlinelibrary.wiley.com/doi/10.1029/2023JG007812, Wiley Online Library.wiley.com/doi/10.1029/2023JG007812, Wiley Online Library.wiley.com/doi/10.1029/2023JG007812, Wiley Online Library.wiley.com/doi/10.1029/2023JG007812, Wiley.com/doi/10.1029/2023JG007812, Wiley.com/

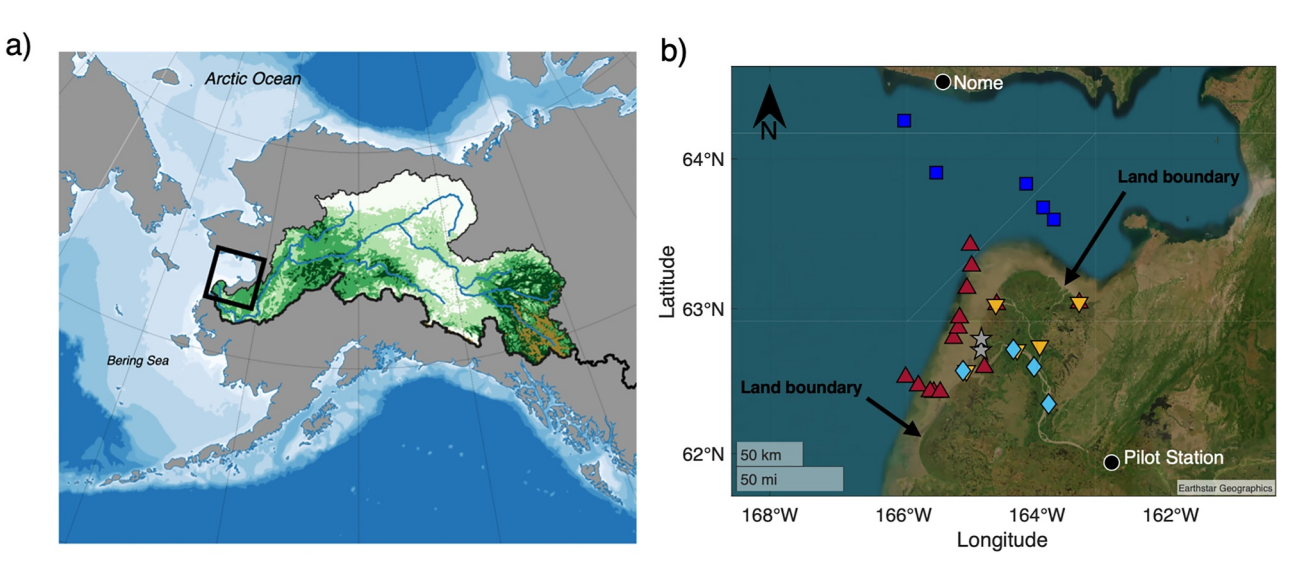


Figure 1. Map of the Yukon River watershed (area outlined by the thin black line) in relation to the Pan-Arctic watershed (area above the thick black line) and the Yukon River land-ocean region sampled in this study (area enclosed in the thick black square) (a; basemap originally published in Kellerman et al. (2023)). The enclosed region is magnified, and sampling locations are noted (b) with a similar color scheme as used in Kellerman et al. (2023). The Yukon land-ocean continuum was sampled during three stages of the hydrograph in 2018–2019: the ascending limb/peak freshet (red filled triangles), the descending limb of freshet (yellow filled inverted triangles), and the late summer (light-blue filled diamonds), including marine samples (salinity > 25 ppt) collected during the ascending limb/peak freshet (dark-blue filled squares) and core riverine samples that were collected during all three stages of the hydrograph (gray filled stars). The villages at Nome and Pilot Station are marked by black filled circles.

ascending limb/peak freshet results in a narrow range of lignin concentrations and compositions across the spatially heterogeneous Yukon River delta, but that high lignin concentrations and associated aromaticity during this stage of the hydrograph drive preferential loss of lignin when compared to the estuarine mixing behavior of the bulk DOC pool.

2. Materials and Methods

2.1. Study Location

The 0.83 million km² Yukon River watershed (Figure 1a) lies within British Columbia, the Canadian Yukon territory, and Alaska. The majority of the watershed is underlain by permafrost, 23% of which is classified as continuous. Vegetation types within the Yukon River Basin include white (*Picea glauca*) and black spruce (*Picea mariana*), quaking aspen (*Populus tremuloides*), paper birch (*Betula papyrifera*), shrubs, and moss hummocks (O'Donnell et al., 2010). Approximate land cover classifications vary between studies but have been reported as 20% shrubland, 40% grassland, 20% forest, and 8% open water and wetlands (Amon et al., 2012). The Yukon River is the third-longest river in the Arctic (3,190 km), and the fifth-largest by annual discharge (208 km³/year). The river delta is located in western Alaska and is distinguished by three major river branches (North, Middle, and South/Main) and two minor river branches (Alakanuk and Emmonak). All Yukon River mouths discharge into the Bering Sea, then flow into the Arctic Ocean through the Bering Strait to the north.

The Yukon River delta was sampled during three distinct stages of the annual hydrograph in 2018 and 2019 (Figure S1 in Supporting Information S1), encompassing peak discharge and low-flow conditions: the ascending limb through the peak of the spring freshet, descending limb of the spring freshet, and late summer (Table S1 in Supporting Information S1, Figure 1b). Delta sampling was restricted to tidally influenced freshwater sites that were at, or upstream of, the major and minor river mouths. Weather and time limitations prevented comprehensive delta sampling across all three stages of the hydrograph, but the Alakanuk and Emmonak river mouths were sampled at all three stages (referred to as "Core riverine" sites, Table S1 in Supporting Information S1) and are isolated to constrain seasonal variation in riverine terrOC concentration and composition (n = 2 freshwater sites during the ascending limb/peak freshet and descending limb, n = 3 during the late summer). Additional, spatially variable, delta sites were sampled across the three stages of the hydrograph (referred to as "Additional riverine" sites, Table S1 in Supporting Information S1) and are used to assess spatial and seasonal variability measured

BURNS ET AL. 3 of 17

within (n = 3 freshwater sites during the ascending limb/peak freshet, n = 5 freshwater sites during the descending limb, n = 4 freshwater sites during the late summer).

During the ascending limb/peak freshet, there was also sampling along two spatially distinct salinity transects (n = 11) in the river plume and into marine waters (salinity >25 ppt) of Norton Sound (n = 5, Figure 1b). While a subset of river plume and marine samples were collected post-peak freshet outflow measured at Pilot Station (Y23-33 in Table S1 of Supporting Information S1), they are representative of terrestrial material transported by the Yukon River during ascending limb/peak freshet conditions based on model-estimated transport times to the mouth of the South/Main river branch (\sim 3 days) and Norton Sound (\sim 21 days) (Clark et al., 2022). No salinity transects were sampled during the descending limb due to weather conditions. One salinity transect was sampled during the late summer (n = 5, Y4-8 in Table 1), as discussed in Novak et al. (2022) and Kellerman et al. (2023), but the samples were not analyzed for lignin due to volume limitations and are therefore not discussed further in this text.

2.2. Sample Collection

Surface water was filtered from the top 10 cm of the water column using a peristaltic pump, acid-washed silicone tubing, and 0.45 μ m Geotech dispos-a-filter Versapor® filter capsules. Filter capsules were rinsed with sample water before sample collection. Samples for lignin analysis were collected in acid-washed and sample-rinsed polycarbonate or high-density polyethylene (HDPE) bottles and stored frozen (<0°C) in the dark until analysis at Texas A&M University at Galveston. Samples for DOC analysis were collected in acid-washed and sample-rinsed polycarbonate or HDPE bottles and stored frozen (<0°C) in the dark until analysis at Florida State University or NASA Goddard Space Flight Center (GSFC) as described in Kellerman et al. (2023) and Novak et al. (2022). Samples for CDOM analysis were collected in pre-combusted amber glass vials and stored cold (~4°C) in the dark until analysis at NASA GSFC as described in Novak et al. (2022). Suspended particulate matter (SPM) was measured by filtering a homogenized volume of sample onto pre-weighed and pre-combusted glass fiber filters. Filters were dried, reweighed, and SPM was calculated by weight difference as described in Kellerman et al. (2023) and Novak et al. (2022). Salinity was measured in situ at the time of sample collection using a Seabird SBE25.

2.3. Lignin Phenols Analysis

Samples were thawed to room temperature and preparation volumes were calculated to allow for 30 μg DOC in the chemical oxidation. Aliquots of freshwater and low salinity samples (≤ 5 ppt) were transferred to precombusted glass centrifuge tubes and concentrated using heated vacuum centrifugation. Aliquots of mid-to-high salinity samples (>5 ppt) were acidified to pH 2 using 6 M sulfuric acid (H_2SO_4), passed through 1 g C18 solid-phase extraction (SPE) cartridges using a closed-loop Dionex Autotrace 280 SPE instrument, and eluted with LC-MS grade methanol (Yan & Kaiser, 2018b). Sample extracts were concentrated under argon gas before analysis.

Concentrated samples and sample extracts were redissolved in argon-sparged 1.1 M sodium hydroxide (NaOH) and transferred to Teflon reaction vials for copper sulfate (CuSO₄) oxidation (2 hr at 150°C) (Yan & Kaiser, 2018a, 2018b). Oxidized samples were immediately spiked with 13 C-labeled internal standards, acidified to pH 2 with 6 M H₂SO₄, and purified using 30 mg hydrophilic-lipophilic balanced SPE cartridges. Lignin phenols in purified samples were detected using ultra-high performance liquid chromatography coupled to mass spectrometry (UHPLC-MS) with electrospray-ionization (ESI). The mass spectrometer was operated using dynamic Multiple Reaction Monitoring with alternating positive and negative modes. Samples were quantified against a five-point standard calibration curve ranging from 0 to 7 μ M for each compound of interest.

2.4. Conservative Mixing Calculations

Conservative mixing was modeled for DOC and lignin at the Yukon River land-ocean interface during the ascending limb/peak freshet. During this period, conservative mixing is shown as a salinity-dependent linear regression between 0.08 ppt (South/Main mouth) to 29.06 ppt (most saline marine sample). For each sample, the percent error was calculated between the (expected) linear conservative mixing estimate and (actual) measured DOC or lignin concentration.

BURNS ET AL. 4 of 17

Table 1

Bulk Physical, Chemical, and Optical Properties Across the Yukon River Land-Ocean Continuum

Station	Date collected	Hydrograph stage	Sample category	Salinity (ppt)	SPM (mg/L)	DOC (mg/L)	$\Sigma_6 \ (\mu g/L)$	Σ_8 (µg/L)	$\Lambda_6 \text{ (mg/} 100 \text{ mg OC)}$	$\Lambda_8 \text{ (mg/}$ 100 mg OC)	a_{350} (m ⁻¹)	$a_{412} (m^{-1})$
Y1		Late summer	Core riverine	0.14	572.8	3.22	4.27	4.80	0.13	0.15	4.90	1.51
Y2		Late summer	Additional riverine	0.14	436.4	3.51	4.80	5.44	0.14	0.15	5.38	1.70
Y3		Late summer	Additional riverine	0.14	373.8	3.56	6.75	7.48	0.19	0.21	6.18	1.97
Y4	29 August 2018	Late summer	Estuary	14.46	21.8	2.39	n.d.	n.d.	n.d.	n.d.	3.07	1.05
Y5	29 August 2018	Late summer	Estuary	22.04	15.2	1.85	n.d.	n.d.	n.d.	n.d.	1.87	0.63
Y6	30 August 2018	Late summer	Estuary	6.24	119.7	2.92	n.d.	n.d.	n.d.	n.d.	4.27	1.42
Y7	30 August 2018	Late summer	Estuary	2.69	353.1	3.34	n.d.	n.d.	n.d.	n.d.	4.53	1.46
Y8	30 August 2018	Late summer	Estuary	0.78	343.9	3.61	n.d.	n.d.	n.d.	n.d.	5.20	1.66
Y9	31 August 2018	Late summer	Core riverine	0.13	459.4	4.92	8.00	8.79	0.16	0.18	7.83	2.57
Y10	31 August 2018	Late summer	Core riverine	0.13	422.5	4.85	15.15	21.41	0.31	0.44	7.82	2.49
Y11	31 August 2018	Late summer	Additional riverine	0.13	461.7	4.78	7.34	8.20	0.15	0.17	7.86	2.50
Y12	31 August 2018	Late summer	Additional riverine	0.13	388.5	4.63	9.03	10.08	0.19	0.22	7.82	2.49
Y13	30 May 2019	Ascending limb/peak	Estuary	15.13	n.d.	5.34	11.83	12.13	0.22	0.23	8.87	3.19
Y14	30 May 2019	Ascending limb/peak	Estuary	13.24	n.d.	6.23	28.24	30.29	0.45	0.49	11.02	3.98
Y15	30 May 2019	Ascending limb/peak	Estuary	3.90	n.d.	9.52	73.48	76.82	0.77	0.81	19.48	7.21
Y16	30 May 2019	Ascending limb/peak	Estuary	5.10	n.d.	8.02	33.55	36.22	0.42	0.45	17.59	6.46
Y17	30 May 2019	Ascending limb/peak	Estuary	1.60	n.d.	10.76	78.84	82.44	0.73	0.77	21.13	7.86
Y18	31 May 2019	Ascending limb/peak	Additional riverine	0.08	n.d.	9.88	89.02	95.46	0.90	0.97	24.54	9.29
Y19	31 May 2019	Ascending limb/peak	Additional riverine	0.08	n.d.	11.94	65.09	68.67	0.55	0.58	22.24	8.21
Y20	1 June 2019	Ascending limb/peak	Core riverine	0.08	n.d.	11.34	77.33	81.36	0.68	0.72	21.75	8.02
Y21	1 June 2019	Ascending limb/peak	Core riverine	0.08	n.d.	10.19	81.95	86.20	0.80	0.85	21.51	7.91
Y22	2 June 2019	Ascending limb/peak	Additional riverine	0.08	n.d.	11.60	70.71	75.11	0.61	0.65	21.02	7.65
Y23	9 June 2019	Ascending limb/peak	Marine	29.06	2.1	1.28	0.37	0.40	0.03	0.03	0.66	0.27
Y24	10 June 2019	Ascending limb/peak	Marine	28.09	n.d.	1.44	1.06	1.09	0.07	0.08	0.76	0.25

BURNS ET AL. 5 of 17

Table 1

Continued												
Station	Date collected	Hydrograph stage	Sample category	Salinity (ppt)	SPM (mg/L)	DOC (mg/L)	$\Sigma_6 \ (\mu g/L)$	$\begin{array}{c} \Sigma_8 \\ (\mu g/L) \end{array}$	$\Lambda_6 ({ m mg/} 100 { m mg OC})$	$\Lambda_8 \text{ (mg/} 100 \text{ mg OC)}$	$a_{350} (m^{-1})$	$a_{412} (m^{-1})$
Y25	10 June 2019	Ascending limb/peak	Estuary	2.51	63.6	8.39	44.06	46.40	0.53	0.55	17.26	6.58
Y26	10 June 2019	Ascending limb/peak	Estuary	0.30	n.d.	9.35	47.78	50.64	0.51	0.54	17.79	6.38
Y27	10 June 2019	Ascending limb/peak	Estuary	3.70	45.8	9.17	37.53	39.54	0.41	0.43	17.45	6.41
Y28	11 June 2019	Ascending limb/peak	Estuary	0.24	91.0	9.31	60.02	63.26	0.64	0.68	17.70	6.35
Y29	11 June 2019	Ascending limb/peak	Estuary	5.10	39.0	8.92	52.16	55.89	0.58	0.63	16.34	5.93
Y30	11 June 2019	Ascending limb/peak	Estuary	7.61	16.0	8.39	14.01	14.50	0.17	0.17	14.92	5.44
Y31	11 June 2019	Ascending limb/peak	Marine	26.99	1.8	1.91	2.15	2.28	0.11	0.12	1.68	0.58
Y32	11 June 2019	Ascending limb/peak	Marine	28.34	2.0	1.50	0.93	1.02	0.06	0.07	1.03	0.36
Y33	11 June 2019	Ascending limb/peak	Marine	28.50	2.7	1.39	0.34	0.36	0.02	0.03	0.64	0.22
Y34	26 June 2019	Descending limb	Additional riverine	0.11	58.0	6.64	31.19	34.79	0.47	0.52	16.81	6.06
Y35	26 June 2019	Descending limb	Additional riverine	0.11	91.3	6.41	41.31	46.08	0.64	0.72	13.52	4.69
Y36	27 June 2019	Descending limb	Additional riverine	0.11	81.4	6.38	23.88	26.61	0.37	0.42	13.96	4.87
Y37	27 June 2019	Descending limb	Core riverine	0.11	135.9	6.33	45.15	56.43	0.71	0.89	13.32	4.63
Y38	28 June 2019	Descending limb	Core riverine	0.11	123.0	6.24	20.23	22.33	0.32	0.36	14.38	5.07
Y39	28 June 2019	Descending limb	Additional riverine	0.11	73.3	6.32	19.13	21.31	0.30	0.34	13.90	4.86
Y40	29 June 2019	Descending limb	Additional riverine	0.11	81.3	6.22	25.54	27.99	0.41	0.45	13.12	4.71

Note. Sample numbering scheme replicated from Kellerman et al. (2023). Salinity (from Kellerman et al. (2023)); SPM: suspended particulate matter (from Kellerman et al. (2023)); DOC: dissolved organic carbon (from Kellerman et al. (2023)); Σ_6 : sum of six vanillyl and syringyl phenols; Σ_8 : sum of eight vanillyl, syringyl, and cinnamyl phenols; Λ_6 : sum of six lignin phenols normalized to DOC concentration; Λ_8 : sum of eight lignin phenols normalized to DOC concentration; α_{350} : absorbance at 350 nm (from Kellerman et al. (2023)); α_{412} : absorbance at 412 nm; n.d.: no data available.

3. Results and Discussion

3.1. Seasonality of Riverine Physical and Chemical Signature

To evaluate seasonal and spatial variability in terrOC composition within the Yukon River delta, we quantified lignin phenols and compound class ratios (Table S2 in Supporting Information S1) for samples collected across the entire delta ("Core riverine" and "Additional riverine" in Tables 1 and 2) during three stages of the annual hydrograph: ascending limb/peak freshet (n = 5), descending limb (n = 7), and late summer (n = 7; Tables 1 and 2). Seasonal transitions were captured at the Emmonak and Alakanuk stations ("Core riverine" in Tables 1 and 2), both sampled during all three stages of the annual hydrograph. DOC concentration and the carbon-normalized sum of eight syringyl, vanillyl, and cinnamyl phenols (Λ_8) were positively correlated to riverine discharge, with the highest concentrations measured during the ascending limb/peak freshet and the lowest concentrations measured during the late summer (Figures 2a and 2b). During the ascending limb/peak freshet, lignin compound class ratios included low p-hydroxy-to-vanillyl phenol ratios (P:V, Figure 2c), low syringyl-to-vanillyl phenol

BURNS ET AL. 6 of 17

 Table 2

 Source-Specific Lignin Composition Across the Yukon River Land-Ocean Continuum

Source-Specific Lignin Composition Across the Yukon River Land-Ocean Continuum										
Station	Date collected	Hydrograph stage	Sample category	$\Lambda_{\rm V}$ (mg/100 mg OC)	P:V	C:V	S:V	Pn:P	$\mathrm{Ad:Al}_{\mathrm{V}}$	Ad:Al _S
Y1	27 August 2018	Late summer	Core riverine	0.10	2.12	0.17	0.36	0.28	0.71	0.38
Y2	28 August 2018	Late summer	Additional riverine	0.09	1.85	0.20	0.47	0.30	0.74	0.58
Y3	28 August 2018	Late summer	Additional riverine	0.14	1.32	0.14	0.34	0.31	0.75	0.65
Y4	29 August 2018	Late summer	Estuary	n.d.	n.d.	n.d.	n.d.	n.d.	n.d.	n.d.
Y5	29 August 2018	Late summer	Estuary	n.d.	n.d.	n.d.	n.d.	n.d.	n.d.	n.d.
Y6	30 August 2018	Late summer	Estuary	n.d.	n.d.	n.d.	n.d.	n.d.	n.d.	n.d.
Y7	30 August 2018	Late summer	Estuary	n.d.	n.d.	n.d.	n.d.	n.d.	n.d.	n.d.
Y8	30 August 2018	Late summer	Estuary	n.d.	n.d.	n.d.	n.d.	n.d.	n.d.	n.d.
Y9	31 August 2018	Late summer	Core riverine	0.13	1.92	0.12	0.25	0.25	0.79	0.19
Y10	31 August 2018	Late summer	Core riverine	0.20	1.84	0.65	0.57	0.21	0.50	0.20
Y11	31 August 2018	Late summer	Additional riverine	0.11	1.81	0.16	0.38	0.30	0.77	0.50
Y12	31 August 2018	Late summer	Additional riverine	0.14	1.76	0.16	0.34	0.27	0.69	0.39
Y13	30 May 2019	Ascending limb/peak	Estuary	0.16	0.63	0.04	0.37	0.27	0.89	0.76
Y14	30 May 2019	Ascending limb/peak	Estuary	0.31	0.68	0.10	0.44	0.25	1.01	0.69
Y15	30 May 2019	Ascending limb/peak	Estuary	0.59	0.37	0.06	0.30	0.40	0.65	0.53
Y16	30 May 2019	Ascending limb/peak	Estuary	0.28	0.44	0.12	0.48	0.29	1.03	0.68
Y17	30 May 2019	Ascending limb/peak	Estuary	0.54	0.63	0.06	0.35	0.27	0.95	0.70
Y18	31 May 2019	Ascending limb/peak	Additional riverine	0.64	0.60	0.10	0.40	0.45	0.68	0.48
Y19	31 May 2019	Ascending limb/peak	Additional riverine	0.42	0.57	0.07	0.30	0.23	0.82	0.41
Y20	1 June 2019	Ascending limb/peak	Core riverine	0.53	0.58	0.07	0.30	0.26	0.72	0.48
Y21	1 June 2019	Ascending limb/peak	Core riverine	0.61	0.40	0.07	0.32	0.36	0.74	0.49
Y22	2 June 2019	Ascending limb/peak	Additional riverine	0.46	0.61	0.08	0.32	0.24	0.73	0.61
Y23	9 June 2019	Ascending limb/peak	Marine	0.02	1.36	0.13	0.43	0.32	1.15	0.63
Y24	10 June 2019	Ascending limb/peak	Marine	0.06	0.49	0.04	0.32	0.28	1.33	0.71
Y25	10 June 2019	Ascending limb/peak	Estuary	0.38	0.48	0.07	0.38	0.35	0.76	0.41
Y26	10 June 2019	Ascending limb/peak	Estuary	0.38	0.69	0.08	0.33	0.23	0.76	0.38
Y27	10 June 2019	Ascending limb/peak	Estuary	0.32	0.42	0.07	0.29	0.38	0.76	0.38
Y28	11 June 2019	Ascending limb/peak	Estuary	0.49	0.50	0.07	0.32	0.38	0.59	0.52
Y29	11 June 2019	Ascending limb/peak	Estuary	0.39	0.56	0.11	0.49	0.33	0.82	0.61
Y30	11 June 2019	Ascending limb/peak	Estuary	0.13	0.73	0.05	0.30	0.13	1.77	0.85
Y31	11 June 2019	Ascending limb/peak	Marine	0.09	0.60	0.08	0.29	0.36	0.97	0.68
Y32	11 June 2019	Ascending limb/peak	Marine	0.05	1.09	0.12	0.31	0.38	1.12	0.67
Y33	11 June 2019	Ascending limb/peak	Marine	0.02	1.85	0.08	0.33	0.37	1.16	0.48
Y34	26 June 2019	Descending limb	Additional riverine	0.31	1.07	0.18	0.51	0.47	0.55	0.48
Y35	26 June 2019	Descending limb	Additional riverine	0.43	0.72	0.17	0.48	0.46	0.41	0.41
Y36	27 June 2019	Descending limb	Additional riverine	0.26	1.31	0.16	0.42	0.27	0.93	0.41
Y37	27 June 2019	Descending limb	Core riverine	0.40	0.99	0.45	0.80	0.21	0.45	0.26
Y38	28 June 2019	Descending limb	Core riverine	0.22	1.29	0.15	0.49	0.31	0.74	0.53
Y39	28 June 2019	Descending limb	Additional riverine	0.21	1.37	0.17	0.46	0.29	0.70	0.50
Y40	29 June 2019	Descending limb	Additional riverine	0.29	1.42	0.13	0.39	0.30	0.55	0.42

Note. Sample numbering scheme replicated from Kellerman et al. (2023). Λ_V : vanillyl phenols normalized to DOC concentration; P:V: ratio of p-hyroxy-to-vanillyl phenols; C:V: ratio of cinnamyl-to-vanillyl phenols; S:V: ratio of syringyl-to-vanillyl phenols; Pn:P: ratio of p-hydroxyacetophenone-to-total p-hydroxy phenols; Ad: Al_V: ratio of acid-to-aldehyde vanillyl phenols; Ad:Al_S: ratio of acid-to-aldehyde syringyl phenols; n.d.: no data available.

BURNS ET AL. 7 of 17

21698961, 2024, 6, Downloaded from https://agupubs.onlinelibrary.wiley.com/doi/10.1029/2023/G007812, Wiley Online Library on [24/08/2024]. See the Terms and Conditions (https://onlinelibrary.wiley.com/terms-and-conditions) on Wiley Online Library for rules of use; OA articles

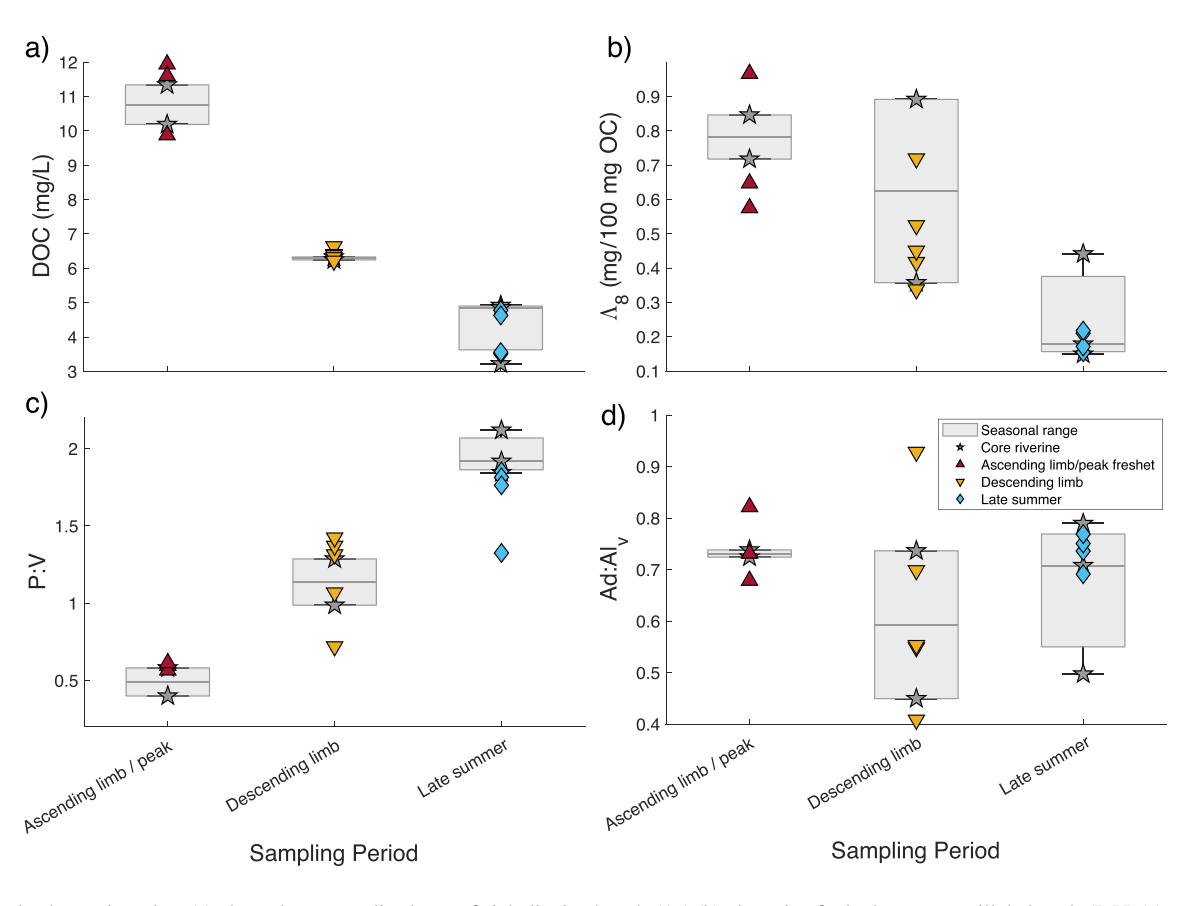


Figure 2. Dissolved organic carbon (a), the carbon-normalized sum of eight lignin phenols (Λ_8) (b), the ratio of p-hydroxy-to-vanillyl phenols (P:V) (c), and the ratio of acid-to-aldehyde vanillyl phenols (Ad:Al_V) (d) measured at freshwater Yukon delta sites during three stages of the hydrograph. Seasonal changes (box-and-whisker plots) are shown for the core riverine sites (Alakanuk and Emmonak channel mouths, gray filled stars) sampled during each stage of the hydrograph. Results from additional, spatially variable delta samples (excluding the core riverine sites) collected during the ascending limb/peak freshet (red filled stars), descending limb (yellow filled inverted triangles), and late summer (light-blue filled diamonds) are also shown.

ratios (S:V, Figure 3d), low cinnamyl-to-vanillyl phenol ratios (C:V, Figure 3c), high carbon-normalized vanillyl phenol yields (high Λ_V , Figure 3a), and a narrow range of vanillyl acid-to-aldehyde ratios (Ad:Al $_V$, Figure 2d). During the descending limb and late summer, compared to the ascending limb, lignin compound class ratios included continually increasing P:V (Figure 2c), higher and more spatially-variable C:V and S:V (Figures 3c and 3d), continually decreasing Λ_V (Figure 3a), and more spatially-variable Ad:Al $_V$ (Figure 2d). These results suggest that riverine DOC is dominated by young vascular plant sources primarily comprised of woody tissues and gymnosperm plant types during the ascending limb/peak freshet but is more spatially variable in terrestrial source contributions and diagenetic state during the descending limb and late summer.

3.1.1. DOC and Lignin Concentration

DOC and lignin concentrations were highest during the ascending limb/peak freshet and lowest during the late summer (Table 1, Figure 2). Riverine DOC concentration at the seasonally sampled ("Core riverine" in Table 1) sites ranged from 10.19–11.34 mg/L during the ascending limb/peak freshet, 6.24–6.33 mg/L during the descending limb, and 3.22–4.92 mg/L during the late summer, whereas DOC across the entire delta ("Core riverine" and "Additional riverine" in Table 1) ranged from 9.88–11.94, 6.22–6.64, and 3.22–4.92 mg/L during the same sampling events (Figure 2a). To quantify the relative terrestrial contribution to the DOC pool, Λ_8 was calculated and seasonally intercompared. Λ_8 at the seasonally sampled ("Core riverine" in Table 1) sites ranged from 0.72–0.85 mg/100 mg OC during the ascending limb/peak freshet, 0.36–0.89 mg/100 mg OC during the descending limb, and 0.15–0.44 mg/100 mg OC during the late summer (Figure 2b), whereas Λ_8 across the entire delta ("Core riverine" and "Additional riverine" in Table 1) ranged from 0.58–0.97, 0.34–0.89, and 0.15–0.44 mg/100 mg OC during the same sampling events (Figure 2b). Based on results from "Core riverine" sites, we

BURNS ET AL. 8 of 17

21698961, 2024, 6, Downloaded from https://agupubs.onlinelibrary.wiley.com/doi/10.1029/2023JG007812, Wiley Online Library on [24/08/2024]. See the Terms and Conditions (https://onlinelibrary.wiley.com/terms-and-conditions) on Wiley Online Library for rules of use; OA articles are governed by the applicable Creative Commons Licenses

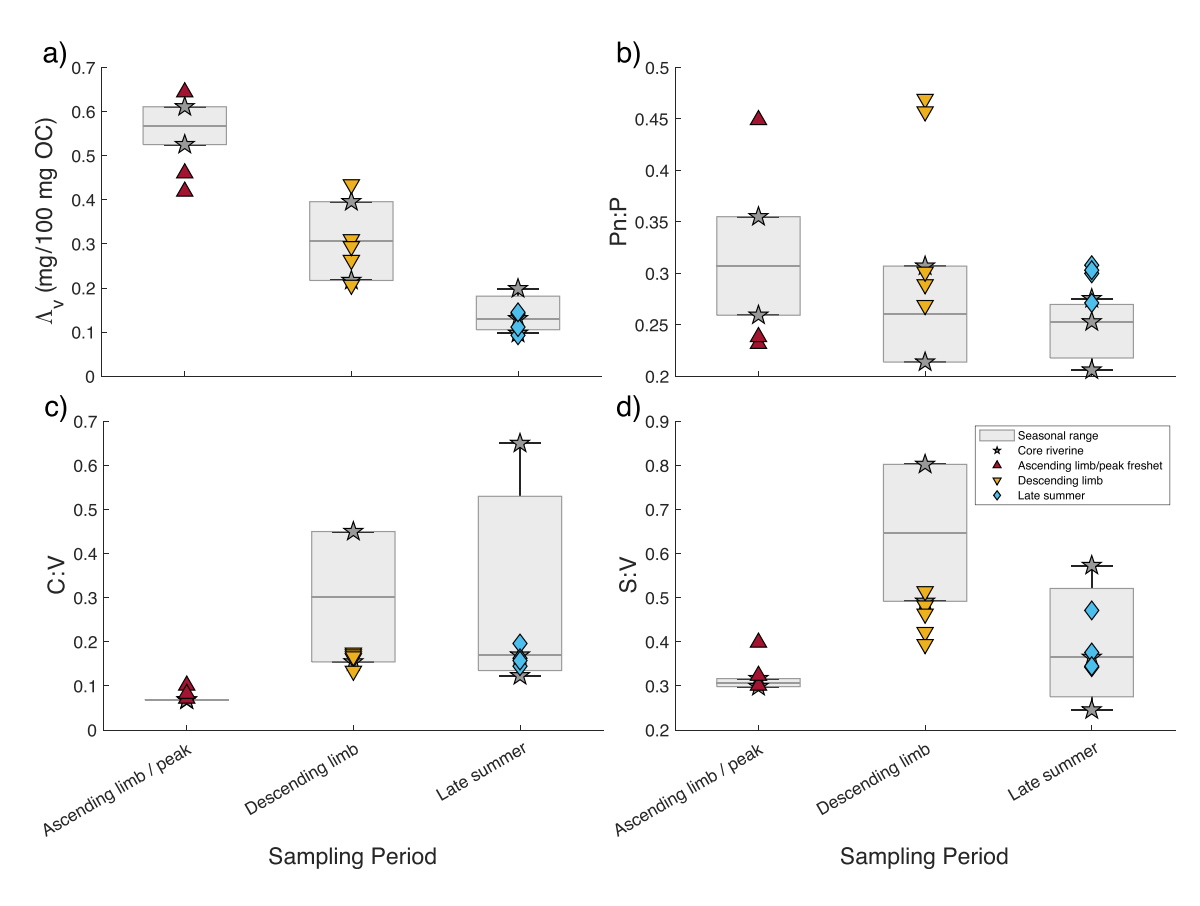


Figure 3. Carbon-normalized vanillyl phenols (Λ_V) (a), the ratio of p-hydroxyacetophenone-to-total p-hydroxy phenols (Pn:P) (b), the ratio of cinnamyl-to-vanillyl phenols (C:V) (c), and the ratio of syringyl-to-vanillyl phenols (S:V) (d) measured at freshwater Yukon delta sites during three stages of the hydrograph. Seasonal changes (box-and-whisker plots) are shown for the core riverine sites (Alakanuk and Emmonak channel mouths, gray filled stars) sampled during each stage of the hydrograph. Results from additional, spatially variable delta samples (excluding the core riverine sites) collected during the ascending limb/peak freshet (red filled stars), descending limb (yellow filled inverted triangles), and late summer (light-blue filled diamonds) are also shown.

generally observed higher terrestrial contribution to the DOC pool during the ascending limb/peak freshet with continual decreases into the descending limb and late summer. This seasonal trend follows that previously observed across the hydrograph at Pilot Station (Mann et al., 2016; Spencer et al., 2008), suggesting that seasonal variability in terrestrial DOC is positively correlated to riverine discharge (*Q*) (Raymond et al., 2007; Spencer et al., 2008).

Spatially variable delta samples ("Core riverine" and "Additional riverine" in Table 1) follow the same dischargecorrelated trend but cannot be attributed to seasonal factors alone. Results from the descending limb and late summer include sites upstream of the river mouths, where most of the ascending limb/peak freshet sampling was focused, suggesting that the increased terrestrial influence during the ascending limb/peak freshet may also be driven by deltaic inputs (e.g., localized runoff from surface soil and litter layers, tributary inputs, riverbank erosion). Deltaic inputs during the ascending limb/peak freshet can be further investigated through the comparison of 2019 ascending limb measurements ($Q = 17,188-17,726 \text{ m}^3/\text{s}$; The Arctic Great Rivers Observatory, 2024) to 2009 ascending limb measurements taken ~200 km upstream at Pilot Station ($Q = 10.874 \text{ m}^3/\text{s}$; Mann et al., 2016), which corresponded to the largest deviation in Λ_8 across the sampled hydrograph. Since Λ_8 is a function of lignin and DOC concentration, the elevated Λ_8 in our study, compared to that observed by Mann et al. (2016), is driven by higher dissolved lignin and lower DOC concentrations. The sum of eight syringyl, vanillyl, and cinnamyl phenols (Σ_8) ranged from 68.67–95.46 µg/L across the entire delta ("Core riverine" and "Additional riverine" in Table 1) during the ascending limb/peak freshet in our study, compared to $62.1~\mu g/L$ measured at Pilot Station by Mann et al. (2016). Additionally, DOC ranged from 9.88-11.94 mg/L across the entire delta ("Core riverine" and "Additional riverine" in Table 1) during the ascending limb/peak freshet in our study, compared to 13.0 mg/L measured at Pilot Station by Mann et al. (2016). Based on spatial differences

BURNS ET AL. 9 of 17

between our delta sites and Pilot Station, the increased Λ_8 measured in this study may be indicative of microbial degradation of biolabile DOC during riverine transport (Holmes et al., 2008), or quantitatively significant downstream riverine or deltaic terrOC inputs. However, temporal variability between these sample sets could be attributed to interannual differences in the magnitude of freshet flow conditions, or climate-related decadal increases in Λ_8 (e.g., due to increased precipitation, land cover changes, coastal erosion) that may be most apparent during high-flow conditions.

3.1.2. Dissolved Lignin Diagenesis and Non-Vascular Sources

To evaluate the diagenetic state and age of DOC within the Yukon River delta, we seasonally intercompared vanillyl and syringyl acid-to-aldehyde ratios (Ad:Al_V and Ad:Al_S) and P:V, respectively. Ad:Al_V and Ad:Al_S are commonly used as diagenetic indicators since lignin phenols are oxidized via photochemical and microbial pathways, leading to higher concentrations of acidic phenols produced through the chemical oxidation procedure (Hedges et al., 1988; Opsahl & Benner, 1995, 1998). Ad:Al_V at the seasonally sampled ("Core riverine" in Table 2) sites ranged from 0.72–0.74 during the ascending limb/peak freshet, 0.45–0.74 during the descending limb, and 0.50-0.79 during the late summer, whereas Ad:Al_V across the entire delta ("Core riverine" and "Additional riverine" in Table 2) ranged from 0.68-0.82, 0.41-0.93, and 0.50-0.79 during the same sampling events (Figure 2d). Ad:Al_s at the seasonally sampled ("Core riverine" in Table 2) sites ranged from 0.48–0.49 during the ascending limb/peak freshet, 0.26-0.53 during the descending limb, and 0.19-0.38 during the late summer, whereas Ad:Al_s across the entire delta ("Core riverine" and "Additional riverine" in Table 2) ranged from 0.41-0.61, 0.26-0.53, and 0.19-0.65 during the same sampling events. All Ad:Al_V and Ad:Al_S fall within confined ranges of 0.41-0.93 and 0.19-0.65, respectively, which are comparable to those measured in the Yenisey (Ad:Al_V = 0.86 and Ad:Al_S = 0.61; Yan & Kaiser, 2018b) and lower-latitude Brazos Rivers (Ad:Al_V = 0.43 and Ad:Al_s = 0.49; Yan & Kaiser, 2018b) and show little indication of seasonally-dependent diagenetic processing. However, the narrow range of Ad:Al_V during the ascending limb/peak freshet suggests that the diagenetic state of riverine terrOC is relatively homogenous throughout the Yukon River delta at that stage of the hydrograph. Overall, while we observed some variability in Ad:Al_V and Ad:Al_S, it is difficult to deduce clear seasonal or spatial trends in riverine terrOC diagenesis using these environmental parameters.

The ratio of P:V has been shown to be positively correlated to DOC age based on an empirical relationship between P:V and Δ^{14} C in Arctic rivers that stems from the overlap of p-hydroxy phenols and aged DOC in peat soils (Amon et al., 2012). P:V at the seasonally sampled ("Core riverine" in Table 2) sites ranged from 0.40–0.58 during the ascending limb/peak freshet, 0.99-1.29 during the descending limb, and 1.84-2.12 during the late summer, whereas P:V across the entire delta ("Core riverine" and "Additional riverine" in Table 2) ranged from 0.40–0.61, 0.72–1.42, and 1.32–2.12 during the same sampling events (Figure 2c). Based on the relationship established by Amon et al. (2012), seasonal samples indicate that the age of riverine DOC increases from the ascending limb/peak freshet to late summer, which can be attributed to deeper hydrologic flow paths in late summer that increase the contribution of aged terrestrial DOC from groundwater and soils (Aiken et al., 2014). P: V ratios measured across the delta in this study were similar to those measured ~200 km upstream at Pilot Station by Amon et al. (2012) in 2003–2007, contrary to expected increases in aged DOC contribution due to permafrost thaw, receding glaciers, and intensified groundwater inputs (Aiken et al., 2014). However, other studies have found that DOC released from thawing permafrost is rapidly utilized by microbes and resembles riverine DOC after a 28-day incubation (Spencer et al., 2015). Therefore, the stable P:V observed in the Yukon River between 2003 and 2019 does not negate the presence of increasing contributions of aged DOC, but highlights the challenge of investigating this environmentally-critical, albeit biolabile, dissolved organic matter (DOM) fraction.

Peats and mosses are enriched in p-hydroxyacetophenone relative to all p-hydroxy phenols, allowing Pn:P ratios to serve as a source indicator to further investigate these non-vascular plant contributions to the system (Williams et al., 1998). Pn:P at the seasonally sampled ("Core riverine" in Table 2) sites ranged from 0.26–0.36 during the ascending limb/peak freshet, 0.21–0.31 during the descending limb, and 0.21–0.28 during the late summer, whereas Pn:P across the entire delta ("Core riverine" and "Additional riverine" in Table 2) ranged from 0.23–0.45, 0.21–0.47, and 0.21–0.31 during the same sampling events (Figure 3b). Our results do not show a clear seasonal trend in the contribution of peat and mosses to riverine terrOC signature but do suggest there is some spatial variation, which may be due to pronounced bank erosion of peat soils at certain sites within the Yukon River delta. Based on an elevated Pn:P ratio for peat (Amon et al., 2012; Williams et al., 1998), we speculate there may be higher peat contributions to riverine DOC at the mouth near the North river branch during the ascending

BURNS ET AL. 10 of 17

limb/peak freshet (Y18 in Table 2) and descending limb (Y34 in Table 2) and the mouth of the Middle river branch (Y35 in Table 2) during the descending limb. Due to limited spatial resolution, it is difficult to determine whether bank erosion occurs at these sites or further upstream. However, these findings do suggest that there may be differences in terrOC composition within and exiting the North and Middle river branches compared to the South/Main river branch (Y36 in Table 2) at certain stages of the hydrograph.

3.1.3. Vascular Plant DOM and Source Variability

To determine vascular plant contribution to terrOC across the annual hydrograph, $\Lambda_{\rm V}$ was calculated and seasonally intercompared. Vanillyl phenols are a consistent component of all lignin heteropolymers, allowing $\Lambda_{\rm V}$ to serve as an indicator of relative vascular plant contribution to the DOC pool and eliminating the uncertainty that stems from variability in syringyl and cinnamyl phenols with terrestrial source and reactivity (Hernes et al., 2007; Opsahl & Benner, 1995; Spencer et al., 2008). $\Lambda_{\rm V}$ at the seasonally sampled ("Core riverine" in Table 2) sites ranged from 0.53–0.61 mg/100 mg OC during the ascending limb/peak freshet, 0.22–0.40 mg/100 mg OC during the descending limb, and 0.10–0.20 mg/100 mg OC during the late summer, whereas $\Lambda_{\rm V}$ across the entire delta ("Core riverine" and "Additional riverine" in Table 2) ranged from 0.42–0.64, 0.21–0.43, and 0.09–0.20 mg/100 mg OC during the same sampling events (Figure 3a). The seasonality of $\Lambda_{\rm V}$ reflects that of $\Lambda_{\rm S}$, with the highest vascular plant contribution to the DOC pool occurring during the ascending limb/peak freshet and continual descreases into the descending limb and late summer, corroborating previous conclusions that the spring freshet is a period of high vascular plant DOM export due to surface runoff and leaching of litter layers (Guo & Macdonald, 2006; Neff et al., 2006; Spencer et al., 2008).

Similar to the seasonal and spatial variability observed for Λ_8 , Λ_V variability cannot be attributed to discharge-related factors alone and suggests that higher vascular plant DOM during the ascending limb/peak freshet may also be driven by deltaic inputs (e.g., localized runoff from surface soil and litter layers, tributary inputs, riverbank erosion). Compared to previous measurements taken ~200 km upstream at Pilot Station in 2005, Λ_V was notably higher during the ascending limb/peak freshet in this study (0.42–0.64 mg/100 mg OC compared to 0.27 mg/ 100 mg OC; Spencer et al., 2008). Along with potential vascular plant inputs from riverine and deltaic sources, differences between these samples can be attributed to interannual variability in freshet flow conditions or climate-related decadal increases in Λ_V (e.g., due to increased precipitation, land cover changes, coastal erosion) that appear to be most apparent during high-flow conditions. While the 2005 freshet may be an anomaly due to record discharge (33,414 m³/s; The Arctic Great Rivers Observatory, 2024), this suggests that riverine discharge is not universally correlated to exported vascular plant DOM. Specifically, decreased residence times during high flow conditions may limit the leaching of litter layers and surface soils—further highlighting the complexity of this dynamic and critical period of the hydrograph as it relates to riverine terrOC composition and associated reactivity (Spencer et al., 2008).

Specific vascular plant contributions to the system include woody and non-woody tissues and angiosperms and gymnosperms plant types which can be elucidated using the ratio of C:V and S:V, respectively (Hedges & Mann, 1979). C:V at the seasonally sampled ("Core riverine" in Table 2) sites ranged from 0.07 during the ascending limb/peak freshet, 0.15-0.45 during the descending limb, and 0.12-0.65 during the late summer, whereas C:V across the entire delta ("Core riverine" and "Additional riverine" in Table 2) ranged from 0.07-0.10, 0.13–0.45, and 0.12–0.65 during the same sampling events (Table 2, Figure 3c). S:V at the seasonally sampled ("Core riverine" in Table 2) sites ranged from 0.30-0.32 during the ascending limb/peak freshet, 0.49-0.80 during the descending limb, and 0.25-0.57 during late summer, whereas S:V across the entire delta ("Core riverine" and "Additional riverine" in Table 2) ranged from 0.30-0.40, 0.39-0.80, and 0.25-0.57 during the same sampling events (Table 2, Figure 3d). C:V and S:V in this study are comparable to those measured ~200 km upstream at Pilot Station by Mann et al. (2016), except for the high C:V (0.65 compared to \sim 0.27) measured at the mouth of the Emmonak river branch (Y10 in Table 2) during late summer. This sample was collected immediately following a heavy rainfall event (discussed extensively in Novak et al., 2022) and suggests that delta sources, particularly non-woody plant types, can have a pronounced effect on localized riverine terrOC composition. In general, vascular plant contributions during the ascending limb/peak freshet appear to be dominated by woody tissues and gymnosperm plant types based on low C:V and S:V, respectively; thereafter, we observe a mixture of non-woody/woody tissues and gymnosperm/angiosperm plant types. Based on variability in riverine terrOC source and composition across the annual hydrograph, there are expected to be differences in the processing and

BURNS ET AL. 11 of 17

21698961, 2024, 6, Downloaded from https://agupubs.onlinelibrary.wiley.com/doi/10.1029/2023JG007812, Wiley Online Library on [24/08/2024]. See the Terms and Conditions (https://agupubs.onlinelibrary.wiley.com/doi/10.1029/2023JG007812, Wiley Online Library on [24/08/2024]. See the Terms and Conditions (https://agupubs.onlinelibrary.wiley.com/doi/10.1029/2023JG007812, Wiley Online Library on [24/08/2024]. See the Terms and Conditions (https://agupubs.onlinelibrary.wiley.com/doi/10.1029/2023JG007812, Wiley Online Library on [24/08/2024]. See the Terms and Conditions (https://agupubs.onlinelibrary.wiley.com/doi/10.1029/2023JG007812, Wiley Online Library on [24/08/2024]. See the Terms and Conditions (https://agupubs.com/doi/10.1029/2023JG007812, Wiley Online Library.wiley.com/doi/10.1029/2023JG007812, Wiley Online Library.

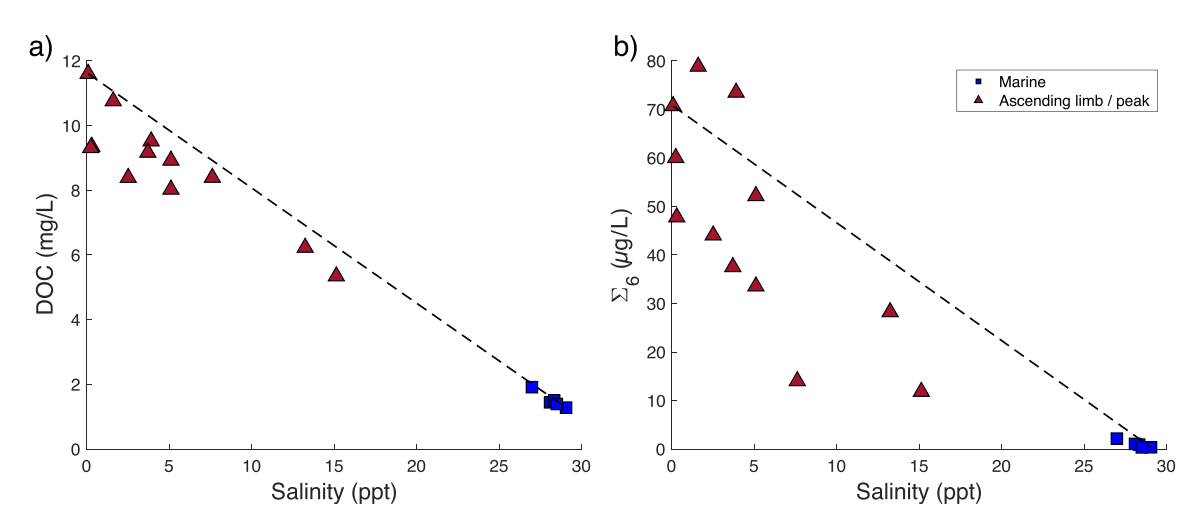


Figure 4. Mixing plots of dissolved organic carbon (DOC) and lignin concentration across salinity in the Yukon River plume (red filled triangles representing Y13–17, Y22, and Y25–30 in Table 1) and into marine waters (dark-blue filled squares representing Y23–24 and Y31–33 in Table 1) during the ascending limb and peak freshet. DOC (a) and the sum of six lignin phenols (Σ_6) (b) are compared to conservative mixing (black dashed line) between the river mouth (0.08 ppt) and the most saline marine location (29.06 ppt).

fate of terrOC during the ascending limb/peak freshet compared to other stages of the hydrograph (Opsahl & Benner, 1995).

3.2. TerrOC Within the Yukon River Estuary

To evaluate terrOC within the Yukon River plume during the ascending limb/peak freshet, DOC and lignin phenols were quantified and compared to linear conservative mixing (Hernes & Benner, 2003) across an environmentally relevant salinity gradient extending from freshwater to high-salinity marine waters. The sum of six syringyl and vanillyl phenols (Σ_6) was used to compare lignin across the salinity gradient, as ester-bound cinnamyl phenols are more prone to diagenetic variability and limit our understanding of terrOC mixing processes (Opsahl & Benner, 1993). DOC and Σ_6 decreased across an estuarine (0.08–15.13 ppt; "Estuary" in Table 1) to marine (26.99–29.06 ppt; "Marine" in Table 1) salinity gradient during the 2019 ascending limb/peak freshet. Compared to DOC, Σ_6 exhibited large variability from linear conservative mixing (Figure 4, Table S3 in Supporting Information S1) that highlights the distinct mixing behavior of DOM compound classes across land-ocean continuums (Kellerman et al., 2023).

To determine the chemical transformation of terrOC within the Yukon River plume, DOC and Σ_6 were plotted against salinity and compared to linear conservative mixing between riverine and marine endmembers (Figure 4, Table S3 in Supporting Information S1). Across the estuarine-to-marine salinity gradient ("Estuary" and "Marine" in Table 1), DOC ranged from 1.28–11.60 mg/L and Σ_6 ranged from 0.34–78.84 μ g/L. The DOC and Σ_6 concentrations measured at the South/Main Yukon River mouth (Y22 in Table 1) were 11.60 mg/L and 70.71 µg/ L, respectively. The DOC and Σ_6 concentrations measured at the highest salinity marine site (Y23 in Table 1) were 1.28 mg/L and 0.37 μg/L, respectively. DOC measured within the plume (0.24–15.13 ppt; "Estuary" in Table 1) was consistently depleted (3%-22%, Table S3 in Supporting Information S1) relative to linear conservative mixing (Figure 4a), whereas Σ_6 exhibited greater variability (Figure 4b). At low salinities, Σ_6 showed minor enrichment relative to linear conservative mixing (18% at 1.6 ppt and 20% at 3.9 ppt, Table S3 in Supporting Information S1), which has been attributed to sediment desorption in previous studies (Hernes & Benner, 2003). However, at all other estuarine salinities, Σ_6 exhibited depletion relative to linear conservative mixing (11%–73%, Table S3 in Supporting Information S1). This deviation from linear conservative mixing suggests that there may be microbial, photochemical, and physical processing within the river plume that preferentially transforms aromatic, lignin-like compounds (e.g., Hernes & Benner, 2003). Due to the high turbidity of the Yukon River during this time of the year, which limits light penetration at depth (Clark et al., 2022), we predict that most of this processing is driven by microbial degradation and the physical transformation of dissolved organic compounds to particulate forms (i.e., flocculation and sedimentation; Hernes & Benner, 2003). At salinity 5.1 ppt (Y16 in Table S3 of Supporting Information S1), the point at which we expect most of this physical

BURNS ET AL. 12 of 17

21698961, 2024, 6, Downloaded from https://agupubs.onlinelibrary.wiley.com/doi/10.1029/2023JG007812, Wiley Online Library on [24/08/2024]. See the Terms and Condition

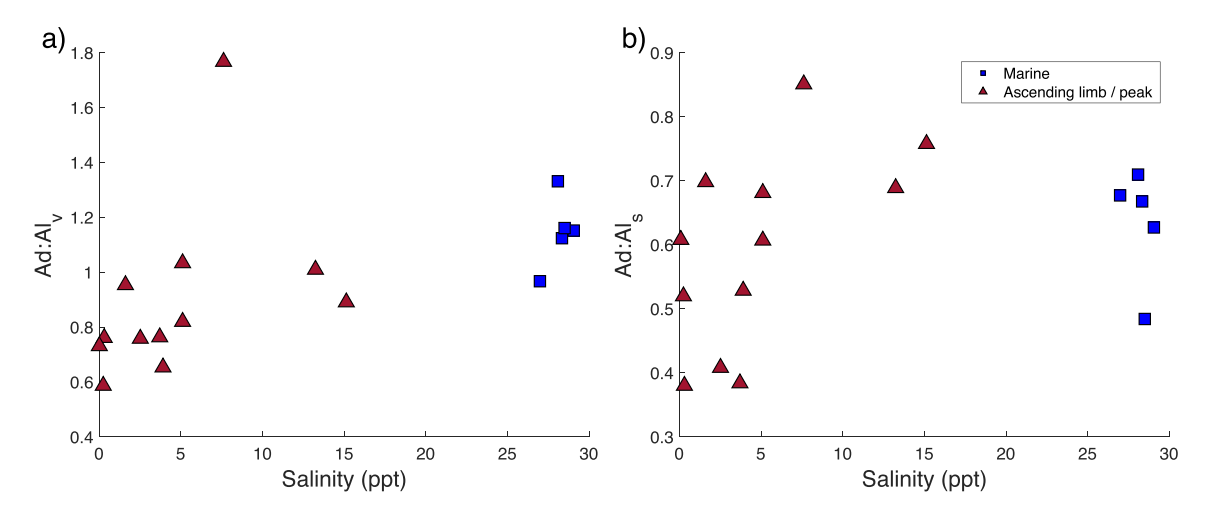


Figure 5. The ratio of acid-to-aldehyde vanillyl (Ad: Al_v) (a) and syringyl phenols (Ad: Al_s) (b) in the Yukon River plume (red filled triangles representing Y13–17, Y22, and Y25–30 in Table 2) and into marine waters (dark-blue filled squares representing Y23–24 and Y31–33 in Table 2) during the ascending limb and peak freshet.

transformation to occur (Clark et al., 2022), we observed 18% depletion in DOC and a 43% depletion in Σ_6 (Table S3 in Supporting Information S1), which highlights the enhanced loss of lignin phenols compared to other dissolved organic compounds. Ultimately, the substantial enrichment and depletion of lignin phenols across the estuarine-to-marine salinity gradient, compared to the bulk DOC pool, suggests that distinct DOM compound classes have wide-ranging reactivities (which may be microbial, photochemical, and physical in nature) (Hernes & Benner, 2003; Kellerman et al., 2023) and necessitate using environmental biomarkers and compositional tools to understand terrOC transformation across Arctic land-ocean continuums.

To assess the salinity-induced diagenesis of the DOC pool, $Ad:Al_V$ and $Ad:Al_S$ were plotted against the sampled salinity gradient (Figure 5). $Ad:Al_V$ ranged from 0.59–1.77 (0.59–1.03 when excluding the abnormally high measurement at Y30) across the estuary ("Estuary" in Table 2) and 0.97–1.33 in the marine waters ("Marine" in Table 2) of Norton Sound (Figure 5a). $Ad:Al_S$ ranged from 0.38–0.85 across the estuary ("Estuary" in Table 2) and 0.48–0.71 in the marine waters ("Marine" in Table 2) of Norton Sound (Figure 5b). $Ad:Al_V$ increased with salinity (Figure 5a), which suggests that the DOC pool is more degraded at higher salinities due to some combination of photochemical, microbial (Hernes & Benner, 2003), and sorption/desorption processes (Hernes et al., 2007). At 7.61 ppt (Y30 in Table 2), specifically, there is a large increase in $Ad:Al_V$ that deviates from the overall trend across the estuarine-to-marine salinity gradient (Figure 5a). The increased degradation of this sample may be connected to the low SPM concentration measured at this location (16.0 mg/L compared to 39.0–91.0 mg/L at other estuarine sites, Table 1) which could allow increased light penetration and photochemical degradation, subsequently affecting microbial processing (Grunert et al., 2021). In that same vein, the relatively low $Ad:Al_S$ observed at 28.5 ppt (Y33 in Table 2, Figure 5b) may be attributed to the higher SPM concentration measured at this location (2.7 mg/L compared to 1.8–2.1 mg/L at other marine sites, Table 1) that could limit light penetration and photochemical degradation.

Generally, terrOC degradation along the Yukon estuarine-to-marine salinity gradient seems to be controlled by water column turbidity and, therefore, may be impacted by several different transformation mechanisms depending on the location within the plume (Clark et al., 2022). In other large river plumes, such as the Mississippi River (Hernes & Benner, 2003), non-conservative depletion of lignin appeared to be dominated by microbial degradation and flocculation in turbid waters below salinity 25 ppt (Ad:Al $_{\rm V}=0.76$ –0.83 and Ad: Al $_{\rm S}=0.64$ –0.80), and photochemical degradation in less turbid waters above salinity 25 ppt (Ad:Al $_{\rm V}=1.02$ –2.70 and Ad:Al $_{\rm S}=0.77$ –2.28). Aside from the high Ad:Al $_{\rm V}$ observed at 7.61 ppt (Y30 in Table 2), no other samples along the Yukon estuarine-to-marine salinity transect suggest photochemically degraded lignin compositions (Ad:Al $_{\rm V}$ and Ad:Al $_{\rm S}=0.77$). While the consistently lower Ad:Al $_{\rm V}$ and Ad:Al $_{\rm S}=0.77$ measured in this study may be partially attributed to methodological differences (Yan & Kaiser, 2018b), we would still expect to see increased Ad:Al $_{\rm V}=0.76$ and Ad:Al $_{\rm S}=0.76$ in the Yukon River plume during the ascending limb/peak freshet seems to be

BURNS ET AL. 13 of 17

21698961, 2024, 6, Downloaded from https://agupubs.onlinelibrary.wiley.com/doi/10.1029/2023JG007812, Wiley Online Library on [24/08/2024]. See the Terms and Conditions (https://agupubs.onlinelibrary.wiley.com/doi/10.1029/2023JG007812, Wiley Online Library on [24/08/2024]. See the Terms and Conditions (https://agupubs.onlinelibrary.wiley.com/doi/10.1029/2023JG007812, Wiley Online Library on [24/08/2024]. See the Terms and Conditions (https://agupubs.onlinelibrary.wiley.com/doi/10.1029/2023JG007812, Wiley Online Library on [24/08/2024]. See the Terms and Conditions (https://agupubs.onlinelibrary.wiley.com/doi/10.1029/2023JG007812, Wiley Online Library on [24/08/2024]. See the Terms and Conditions (https://agupubs.com/doi/10.1029/2023JG007812, Wiley Online Library.wiley.com/doi/10.1029/2023JG007812, Wiley Online Library.

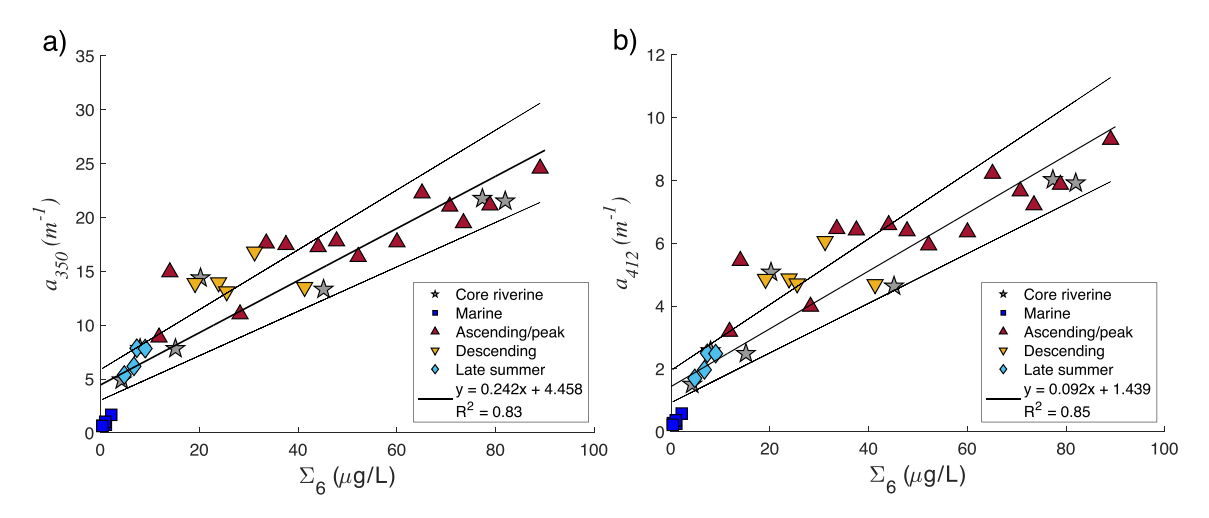


Figure 6. Linear regression (thick black line) and 95% confidence intervals (thin black lines) between the sum of six lignin phenols (Σ_6) and optical indices a_{350} (a) and a_{412} (b) measured across the Yukon land-ocean continuum during three stages of the hydrograph. Core riverine sites (Alakanuk and Emmonak channel mouths) were sampled during each stage of the hydrograph and the results are shown as gray filled stars. Results from additional delta samples (excluding the core riverine sites) are shown as individual points. The ascending/peak data points also include measurements from two salinity transects in the river plume. Marine data points refer to samples with a measured salinity above 25 ppt.

driven by microbial degradation and physical transformation. However, variability in lignin degradation state across the salinity gradient is also connected to the irregular mixing behavior that is known to occur within the Yukon River estuary (Clark & Mannino, 2022). This irregular mixing behavior, which is governed by wind velocity, influences water transport and residence time, impacting where terrestrial material is degraded or settles out of the plume (Clark & Mannino, 2022).

3.3. Projecting terrOC Into Marginal Zones Using Optical Proxies

Challenges with lignin analytical techniques, including long sample preparation times and the need for large sample volumes, highlight the desirability of using optical proxies to determine the concentration and transformation of terrOC within the Yukon River system. Due to the chromophoric nature of terrestrial DOM, light absorption at 350 nm (Hernes & Benner, 2003; Spencer et al., 2008, 2009) and 412 nm (D'Sa & DiMarco, 2009; Novak et al., 2022) have been used to study terrestrial DOC in this and other riverine and near-coastal (\leq 10 ppt) environments. However, while CDOM measurements are robust and simple to perform, there may be marine sources of CDOM that create uncertainty when using absorbance data as an optical proxy for terrestrial DOM across expansive salinity gradients (Chen et al., 2002, 2004). Fortunately, since lignin phenols are derived from terrestrial materials, establishing an empirical relationship between CDOM absorbance and Σ_6 eliminates this analytical uncertainty. Along with the potential for higher sample throughput and improved resolution, an empirical relationship between CDOM and lignin allows for the development of ocean color reflectance algorithms and remote sensing of these terrestrial materials.

Establishing a linear relationship between CDOM absorbance and lignin concentration within our sampling region builds upon the efforts of Kellerman et al. (2023) and Novak et al. (2022) who showed that DOC was linearly related to a_{350} ($R^2 = 0.95$) and a_{412} ($R^2 = 0.95$) across the three stages of the hydrograph and into marine waters. The highest a_{350} was 24.54 m⁻¹ measured in the delta during the ascending limb/peak freshet, whereas the lowest a_{350} was 0.64 m⁻¹ in the marine waters of Norton Sound (Table 1). Similarly, the highest a_{412} was 9.29 m⁻¹ measured in the delta during the ascending limb/peak freshet, whereas the lowest a_{412} was 0.22 m⁻¹ in the marine waters of Norton Sound (Table 1). There is a linear relationship between Σ_6 and a_{350} ($R^2 = 0.83$) as well as Σ_6 and a_{412} ($R^2 = 0.85$) that is seasonally and spatially consistent (Figure 6). However, there are visible deviations from this trend that suggest molar absorptivity is not constant across the Yukon land-ocean continuum. In particular, the measured light-absorbing properties in marine samples are lower than that predicted by linear regression which may be due to decreased SPM concentrations that allow photooxidation to become the primary degradation pathway for optically-active terrestrial materials (Hernes & Benner, 2003). However, lignin phenols are known to be less susceptible than other optically-active compounds to photodegradation due to typically insufficient

BURNS ET AL. 14 of 17

.com/doi/10.1029/2023JG007812, Wiley Online Library on [24/08/2024]. See the Terms and Conditions

Online Library for rules of use; OA articles are governed by the applicable Creative Commons License

transport times (Clark et al., 2022; Opsahl & Benner, 1998) or the chemical resistance of highly processed lignin that ultimately reaches marine waters (Opsahl & Benner, 1998).

Similarly, molar absorptivity and associated compositional changes are known to vary the linear relationship between CDOM absorbance and lignin across river systems and long timescales. For example, the slope of the linear regression between Σ_6 and a_{350} for these samples is 0.242 compared to 0.405 for the Yukon samples in Mann et al. (2016), suggesting that the molar absorptivity of the two sample sets differs based on spatial or temporal factors. Given recent increases in riverine discharge (Tank et al., 2023) and changes to land cover (Frost et al., 2021), among other long-term trends, riverine DOM molar absorptivity may be impacted by climate-related decadal controls. However, we speculate that transport through the river delta also influences the molar absorptivity of the riverine DOM pool. Specifically, upstream riverine sites along the Yukon are more directly influenced by blackwater sources and inputs (Spencer et al., 2008), which may be less quantitatively significant downstream of Pilot Station. Therefore, if CDOM absorbance is to be used as an optical proxy for lignin concentration throughout the Yukon River delta and coastal zone for remote sensing purposes, there is a need for more paired chemical measurements and model improvements that account for variability in molar absorptivity. With future establishment of optical proxies for lignin concentration, additional models can be developed that utilize DOM fluorescence properties to determine lignin compositional variability (i.e., S:V, C:V) across this spatially and temporally heterogeneous system (Hernes et al., 2009; Mann et al., 2016).

4. Conclusions and Future Work

TerrOC cycling within large Arctic rivers and expansive deltas is incredibly complex and simultaneously influenced by spatial and temporal factors. While our lignin results generally follow discharge-correlated seasonal trends established at Pilot Station between the years of 2003–2009, there are notable deviations from previous measurements during the ascending limb/peak freshet. Given the data currently available, it is difficult to discern whether higher lignin concentrations and vascular plant DOM measured in this study are attributed to deltaic inputs downstream of Pilot Station, climate-related decadal increases (e.g., due to increased precipitation, land cover changes, or coastal erosion), or interannual differences in the magnitude and length of freshet conditions. However, we speculate that all spatial and temporal factors controlling terrOC mobilization may be intensified during high-flow conditions. Therefore, compared to previous upstream measurements, the lignin results in this study are considered more representative of terrOC exiting the river mouth during the ascending limb/peak freshet.

Based on the dynamic and intense biogeochemistry of the freshet, along with the scale of land-ocean DOC flux exported to the Bering Sea during the period (approximately 63% of annual DOC flux; Raymond et al., 2007; Spencer et al., 2008), it is evident that there needs to be more intensive sampling during and between separate, historically under-studied, high-flow conditions to improve our understanding of Yukon River terrOC composition and associated DOC reactivity. Across an extensive estuarine-to-marine salinity transect, we observe depletion of terrOC relative to conservative mixing and preferential loss of lignin phenols compared to DOC which appears to be dominated by microbial and physical transformation processes. However, the riverine composition during the ascending limb/peak freshet is chemically distinct compared to other stages of the annual hydrograph (descending limb and late summer), limiting our ability to predict estuarine mixing and transformation of terrOC in entirety. Future studies comparing off-shore lignin concentrations during disparate seasons will improve our understanding of annual land-ocean terrOC flux and distinguish the extent to which riverine composition influences mixing behavior within the plume.

Conflict of Interest

The authors declare no conflicts of interest relevant to this study.

Data Availability Statement

Lignin data can be found in Tables 1 and 2 and accessed through the SeaBASS repository at (Mannino et al., 2024) https://seabass.gsfc.nasa.gov/cruise/Arctic_RSWQ_Yukon_2018, https://seabass.gsfc.nasa.gov/cruise/Arctic_

BURNS ET AL. 15 of 17



Journal of Geophysical Research: Biogeosciences

10.1029/2023JG007812

RSWQ_Yukon_2019a, https://seabass.gsfc.nasa.gov/cruise/Arctic_RSWQ_Yukon_2019b, and https://seabass.gsfc.nasa.gov/cruise/Arctic_RSWQ_Norton_Sound.

Acknowledgments

This work was funded by the NASA Grants (80NSSC18K0492 and 80NSSC22K0152). The authors would like to recognize Edda Mutter and other members of the Yukon River Inter-Tribal Watershed Council for orchestrating the connection with community members in Alakanuk, AK. The fieldwork in Alakanuk, AK was made possible by a number of local Yup'ik collaborators, including Augusta Edmund, Robert and Ragnar Alstrom, Teddy Hamilton, and Sonny Phillip. The authors would also like to recognize Adem Boeckman and Jenefer Bell for their assistance in the fieldwork out of Nome, AK.

References

- Aiken, G. R., Spencer, R. G. M., Striegl, R. G., Schuster, P. F., & Raymond, P. A. (2014). Influences of glacier melt and permafrost thaw on the age of dissolved organic carbon in the Yukon River Basin. Global Biogeochemical Cycles, 28(5), 525–537. https://doi.org/10.1002/ 2013GB004764
- Amon, R. M. W., Rinehart, A. J., Duan, S., Loucharn, P., Prokushkin, A., Guggenberger, G., et al. (2012). Dissolved organic matter sources in large Arctic rivers. *Geochimica et Cosmochimica Acta*, 94, 217–237. https://doi.org/10.1016/j.gca.2012.07.015
- Asmala, E., Bowers, D. G., Autio, R., Kaartokallio, H., & Thomas, D. N. (2014). Qualitative changes in riverine dissolved organic matter at low salinities due to flocculation. *Journal of Geophysical Research: Biogeosciences*, 119(10), 1919–1933. https://doi.org/10.1002/2014JG002722
- Bhatt, U. S., Walker, D. A., Raynolds, M. K., Bieniek, P. A., Epstein, H. E., Comiso, J. C., et al. (2017). Changing seasonality of panarctic tundra vegetation in relationship to climatic variables. *Environmental Research Letters*, 12(5), 055003. https://doi.org/10.1088/1748-9326/aa6b0b
- Box, J. E., Colgan, W. T., Christensen, T. R., Schmidt, N. M., Lund, M., Parmentier, F. W., et al. (2019). Key indicators of Arctic climate change: 1971–2017. Environmental Research Letters, 14(4), 045010. https://doi.org/10.1088/1748-9326/aafc1b
- Chang, G. C., & Dickey, T. D. (2004). Coastal ocean optical influences on solar transmission and radiant heating rate. *Journal of Geophysical Research*, 109(C1), C01020. https://doi.org/10.1029/2003JC001821
- Chen, R. F., Bissett, P., Coble, P., Conmy, R., Gardner, G. B., Moran, M. A., et al. (2004). Chromophoric dissolved organic matter (CDOM) source characterization in the Louisiana Bight. *Marine Chemistry*, 89(1–4), 257–272. https://doi.org/10.1016/j.marchem.2004.03.017
- Chen, R. F., Zhang, Y., Vlahos, P., & Rudnick, S. M. (2002). The fluorescence of dissolved organic matter in the Mid-Atlantic Bight. *Deep Sea Research Part II*, 49(20), 4439–4459. https://doi.org/10.1016/S0967-0645(02)00165-0
- Clark, J. B., & Mannino, A. (2021). Preferential loss of Yukon River delta colored dissolved organic matter under nutrient replete conditions. Limnology & Oceanography, 66(5), 1613–1626. https://doi.org/10.1002/lno.11706
- Clark, J. B., & Mannino, A. (2022). The Impacts of Freshwater Input and Surface Wind Velocity on the Strength and Extent of a Large High Latitude River Plume. Frontiers in Marine Science, 8, 793217. https://doi.org/10.3389/fmars.2021.793217
- Clark, J. B., Mannino, A., Tzortiou, M., Spencer, R. G. M., & Hernes, P. (2022). The Transformation and Export of Organic Carbon Across an Arctic River-Delta-Ocean Continuum. *Journal of Geophysical Research: Biogeosciences*, 127(12), e2022JG007139. https://doi.org/10.1029/2022JG007139
- Cloern, J. E., Canuel, E. A., & Harris, D. (2002). Stable carbon and nitrogen isotope composition of aquatic and terrestrial plants of the San Francisco Bay estuarine system. *Limnology and Oceanography*, 47(3), 713–729. https://doi.org/10.4319/lo.2002.47.3.0713
- D'Sa, E. J., & DiMarco, S. F. (2009). Seasonal variability and controls on chromophoric dissolved organic matter in a large river-dominated coastal margin. *Limnology and Oceanography*, 54(6), 2233–2242. https://doi.org/10.4319/lo.2009.54.6.2233
- Eckard, R. S., Bergamaschi, B. A., Pellerin, B., Spencer, R. G., Dyda, R., & Hernes, P. J. (2020). Organic Matter Integration, Overprinting, and the Relative Fraction of Optically Active Organic Carbon in a Human-Impacted Watershed. Frontiers in Earth Science, 8, 67. https://doi.org/10.
- Eckard, R. S., Hernes, P. J., Bergamaschi, B. A., Stepanauskas, R., & Kendall, C. (2007). Landscape scale controls on the vascular plant component of dissolved organic carbon across a freshwater delta. *Geochimica et Cosmochimica Acta*, 71(24), 5968–5984. https://doi.org/10.1016/j.gca.2007.09.027
- Frost, G. V., Bhatt, U. S., Macander, M. J., Hendricks, A. S., & Jorgenson, M. T. (2021). Is Alaska's Yukon-Kuskokwim Delta Greening or Browning? Resolving Mixed Signals of Tundra Vegetation Dynamics and Drivers in the Maritime Arctic. *Earth Interactions*, 25(1), 76–93. https://doi.org/10.1175/EI-D-20-0025.1
- Grunert, B. K., Tzortziou, M., Neale, P., Menendez, A., & Hernes, P. (2021). DOM degradation by light and microbes along the Yukon River-coastal ocean continuum. Scientific Reports, 11, 10236. https://doi.org/10.1038/s41598-021-89327-9
- Guo, L. D., & Macdonald, R. W. (2006). Source and transport of terrigenous organic matter in the upper Yukon River: Evidence from isotope (δ¹³C, Δ¹⁴C, and δ¹⁵N) composition of dissolved, colloidal, and particulate phases. *Global Biogeochemical Cycles*, 20(2), GB2011. https://doi.org/10.1029/2005GB002593
- Haine, T. W. N., Curry, B., Gerdes, R., Hansen, E., Karcher, M., Lee, C., et al. (2015). Arctic freshwater export: Status, mechanisms, and prospects. Global and Planetary Change, 125, 13–35. https://doi.org/10.1016/j.gloplacha.2014.11.013
- Hedges, J. I., Blanchette, R. A., Weliky, K., & Devol, A. H. (1988). Effects of fungal degradation on the CuO oxidation products of lignin: A controlled laboratory study. Geochimica et Cosmochimica Acta, 52(11), 2717–2726. https://doi.org/10.1016/0016-7037(88)90040-3
- Hedges, J. I., & Mann, D. C. (1979). The characterization of plant tissues by their lignin oxidation products. *Geochimica et Cosmochimica Acta*, 43(11), 1803–1807. https://doi.org/10.1016/0016-7037(79)90028-0
- Hernes, P. J., & Benner, R. (2003). Photochemical and microbial degradation of dissolved lignin phenols: Implications for the fate of terrigenous dissolved organic matter in marine environments. *Journal of Geophysical Research*, 108(C9), 3291. https://doi.org/10.1029/2002JC001421
- Hernes, P. J., Bergamaschi, B. A., Eckard, R. S., & Spencer, R. G. M. (2009). Fluorescence-based proxies for lignin in freshwater dissolved organic matter. *Journal of Geophysical Research*, 114(G4), G00F03. https://doi.org/10.1029/2009JG000938
- Hernes, P. J., Robinson, A. C., & Aufdenkampe, A. K. (2007). Fractionation of lignin during leaching and sorption and implications for organic matter "freshness". Geophysical Research Letters, 34(17), L17401. https://doi.org/10.1029/2007GL031017
- Holmes, R. M., McClelland, J. W., Peterson, B. J., Tank, S. E., Bulygina, E., Eglinton, T. I., et al. (2012). Seasonal and Annual Fluxes of Nutrients and Organic Matter from Large Rivers to the Arctic Ocean and Surrounding Seas. Estuaries and Coasts, 35(2), 369–382. https://doi.org/10. 1007/s12237-011-9386-6
- Holmes, R. M., McClelland, J. W., Raymond, P. A., Frazer, B. B., Peterson, B. J., & Stieglitz, M. (2008). Lability of DOC transported by Alaskan rivers to the Arctic Ocean. Geophysical Research Letters, 35(3), L03402. https://doi.org/10.1029/2007GL032837
- Holmes, R. M., Shiklomanov, A. I., Tank, S. E., McClelland, J. W., & Tretiakov, M. (2015). River Discharge Arctic Report Card: Update for 2015. Retrieved from https://Arctic.noaa.gov/Report-Card/Report-Card-2015/ArtMID/5037/ArticleID/227/River-Discharge
- Kellerman, A. M., Hernes, P. J., McKenna, A. M., Clark, J. B., Edmund, A., Grunert, B., et al. (2023). Mixing behavior of dissolved organic matter at the Yukon and Kolyma land ocean interface. *Marine Chemistry*, 225, 104281. https://doi.org/10.1016/j.marchem.2023.104281
- Mann, P. J., Spencer, R. G. M., Hernes, P. J., Six, J., Aiken, G. R., Tank, S. E., et al. (2016). Pan-Arctic Trends in Terrestrial Dissolved Organic Matter from Optical Measurements. Frontiers in Earth Science, 4, 25. https://doi.org/10.3389/feart.2016.00025

BURNS ET AL. 16 of 17



Journal of Geophysical Research: Biogeosciences

- 10.1029/2023JG007812
- Mannino, A., Tzortziou, M., Hernes, P., Kaiser, K., & Burns, A. (2024). ARCTIC_RSWQ. SeaWiFS Bio-optical Archive and Storage System (SeaBASS) [Dataset]. NASA. https://doi.org/10.5067/SeaBASS/ARCTIC_RSWQ/DATA001
- McClelland, J. W., Holmes, R. M., Peterson, B. J., Raymond, P. A., Striegl, R. G., Zhulidov, A. V., et al. (2016). Particulate organic carbon and nitrogen export from major Arctic rivers. *Global Biogeochemical Cycles*, 30(5), 629–643. https://doi.org/10.1002/2015GB005351
- Meredith, M., Sommerkorn, M., Cassotta, S., Derksen, C., Ekaykin, A., Hollowed, A., et al. (2019). Polar regions. In H.-O. Pörtner, D. C. Roberts, V. Masson-Delmotte, P. Zhai, M. Tignor, E. Poloczanska, et al. (Eds.), IPCC Special Report on the Ocean and Cryosphere in a Changing Climate (pp. 203–320). Cambridge University Press. https://doi.org/10.1017/9781009157964.005
- Neff, J. C., Finlay, J. C., Zimov, S. A., Davydov, S. P., Carrasco, J. J., Schuur, E. A. G., & Davydova, A. I. (2006). Seasonal changes in the age and structure of dissolved organic carbon in Siberian rivers and streams. *Geophysical Research Letters*, 33(23), L23401. https://doi.org/10.1029/2006GL028222
- Novak, M. G., Mannino, A., Clark, J. B., Hernes, P., Tzortziou, M., Spencer, R. G. M., et al. (2022). Arctic biogeochemical and optical properties of dissolved organic matter across river to sea gradients. Frontiers in Marine Science, 9, 949034. https://doi.org/10.3389/fmars.2022.949034
- O'Donnell, J. A., Aiken, G. R., Kane, E. S., & Jones, J. B. (2010). Source water controls on the character and origin of dissolved organic matter in streams of the Yukon River basin, Alaska. *Journal of Geophysical Research*, 115(G3), G03025. https://doi.org/10.1029/2009JG001153
- Opsahl, S., & Benner, R. (1993). Decomposition of senescent blades of the seagrass *Halodule wrightii* in a subtropical lagoon. *Marine Ecology Progress Series*, 94, 191–205. https://doi.org/10.3354/meps094191
- Opsahl, S., & Benner, R. (1995). Early diagenesis of vascular plant tissues: Lignin and cutin decomposition and biogeochemical implications. Geochimica et Cosmochimica Acta, 59(23), 4889–4904. https://doi.org/10.1016/0016-7037(95)00348-7
- Opsahl, S., & Benner, R. (1997). Distribution and cycling of terrigenous dissolved organic matter in the ocean. *Nature*, 386(6624), 480–482. https://doi.org/10.1038/386480a0
- Opsahl, S., & Benner, R. (1998). Photochemical reactivity of dissolved lignin in river and ocean waters. *Limnology and Oceanography*, 43(6), 1297–1304. https://doi.org/10.4319/lo.1998.43.6.1297
- Pegau, W. S. (2002). Inherent optical properties of the central Arctic surface waters. *Journal of Geophysical Research*, 107(C10), 8035. https://doi.org/10.1029/2000JC000382
- Polimene, L., Torres, R., Powley, H. R., Bedington, M., Juhls, B., Palmtag, J., et al. (2022). Biological lability of terrestrial DOM increases CO₂ outgassing across Arctic shelves. *Biogeochemistry*. 160(3), 289–300. https://doi.org/10.1007/s10533-022-00961-5
- Rantanen, M., Karpechko, A. Y., Lipponen, A., Nordling, K., Hyvärinen, O., Ruosteenoja, K., et al. (2022). The Arctic has warmed nearly four times faster than the globe since 1979. *Nature*, 3(1), 168. https://doi.org/10.1038/s43247-022-00498-3
- Rapaic, M., Brown, R., Markovic, M., & Chaumont, D. (2015). An Evaluation of Temperature and Precipitation Surface-Based and Reanalysis Datasets for the Canadian Arctic, 1950–2010. Atmosphere-Ocean, 53(3), 283–303. https://doi.org/10.1080/07055900.2015.1045825
- Rawlins, M. A., Steele, M., Holland, M. M., Adam, J. C., Cherry, J. E., Francis, J. A., et al. (2010). Analysis of the Arctic System for Freshwater
- Cycle Intensification: Observations and Expectations. Journal of Climate, 23(21), 5715–5737. https://doi.org/10.1175/2010JCL13421.1
- Raymond, P. A., McClelland, J. W., Holmes, R. M., Zhulidov, A. V., Mull, K., Peterson, B. J., et al. (2007). Flux and age of dissolved organic carbon exported to the Arctic Ocean: A carbon isotopic study of the five largest arctic rivers. Global Biogeochemical Cycles, 21(4), GB4011. https://doi.org/10.1029/2007GB002934
- Schuur, E. A. G., McGuire, A. D., Schädel, C., Grosse, G., Harden, J. W., Hayes, D. J., et al. (2015). Climate change and the permafrost carbon feedback. *Nature*, 520(7546), 171–179. https://doi.org/10.1038/nature14338
- Sholkovitz, E. R. (1976). Flocculation of dissolved organic and inorganic matter during the mixing of river water and seawater. *Geochemica et Cosmochimica Acta*, 40(7), 831–845. https://doi.org/10.1016/0016-7037(76)90035-1
- Spencer, R. G. M., Aiken, G. R., Butler, K. D., Dornblaser, M. M., Striegl, R. G., & Hernes, P. J. (2009). Utilizing chromophoric dissolved organic matter measurements to derive export and reactivity of dissolved organic carbon exported to the Arctic Ocean: A case study of the Yukon River, Alaska. *Geophysical Research Letters*, 36(6), L06401. https://doi.org/10.1029/2008GL036831
- Spencer, R. G. M., Aiken, G. R., Wickland, K. P., Striegl, R. G., & Hernes, P. J. (2008). Seasonal and spatial variability in dissolved organic matter quantity and composition from the Yukon River basin, Alaska. *Global Biogeochemical Cycles*, 22(4), 1–13. https://doi.org/10.1029/2008GB003231
- Spencer, R. G. M., Mann, P. J., Dittmar, T., Eglinton, T. I., McIntyre, C., Holmes, R. M., et al. (2015). Detecting the signature of permafrost thaw in Arctic rivers. *Geophysical Research Letters*, 42(8), 2830–2835. https://doi.org/10.1002/2015GL063498
- Striegl, R. G., Aiken, G. R., Dornblaser, M. M., Raymond, P. A., & Wickland, K. P. (2005). A decrease in discharge-normalized DOC export by the Yukon River during summer through autumn. *Geophysical Research Letters*, 32(21), L21413. https://doi.org/10.1029/2005GL024413
- Tank, S. E., McClelland, J. W., Spencer, R. G. M., Shiklomanov, A. I., Suslova, A., Moatar, F., et al. (2023). Recent trends in the chemistry of major northern rivers signal widespread Arctic change. *Nature Geoscience*, 16(9), 789–796. https://doi.org/10.1038/s41561-023-01247-7
- The Arctic Great Rivers Observatory. (2024). Discharge Dataset, Version 20231204. Retrieved from https://www.arcticgreatrivers.org/data
- Vonk, J. E., Mann, P. J., Davydov, S., Davydova, A., Spencer, R. G. M., Schade, J., et al. (2013). High biolability of ancient permafrost upon thaw. Geophysical Research Letters, 40(11), 2689–2693. https://doi.org/10.1002/grl.50348
- Ward, C. P., Nalven, S. G., Crump, B. C., Kling, G. W., & Cory, R. M. (2017). Photochemical alteration of organic carbon draining permafrost soils shifts microbial metabolic pathways and stimulates respiration. *Nature Communications*, 8, 772. https://doi.org/10.1038/s41467-017-00759-2
- Williams, C. J., Yavitt, J. B., Kelman Wieder, R., & Cleavitt, N. L. (1998). Cupric oxide oxidation products of northern peat and peat-forming plants. *Canadian Journal of Botany*, 76(1), 51–62. https://doi.org/10.1139/b97-150
- Yan, G., & Kaiser, K. (2018a). A rapid and sensitive method for the analysis of lignin phenols in environmental samples using ultra-high performance liquid chromatography-electrospray ionization-tandem mass spectrometry with multiple reaction monitoring. Analytica Chimica Acta, 1023, 74–80. https://doi.org/10.1016/j.aca.2018.03.054
- Yan, G., & Kaiser, K. (2018b). Ultralow Sample Volume Cupric Sulfate Oxidation Method for the Analysis of Dissolved Lignin. Analytical Chemistry, 90(15), 9289–9295. https://doi.org/10.1021/acs.analchem.8b01867

BURNS ET AL. 17 of 17